Environmental Science
Water Research & Technology

Labile Carbon Release from Oxic-Anoxic Cycling in Woodchip Bioreactors Enhances Nitrate Removal without Increasing Nitrous Oxide Accumulation

Journal:	*Environmental Science: Water Research & Technology*
Manuscript ID	EW-ART-06-2021-000446.R1
Article Type:	Paper

Oxic-anoxic cycling has been identified as a practical method to overcome carbon-limited conditions in denitrifying woodchip bioreactors treating agricultural tile drainage, but the effects of these water management practices on production of the greenhouse gas nitrous oxide (N_2O) have not been evaluated. Here, we use laboratory-scale bioreactors to show that oxic-anoxic cycling significantly enhances nitrate removal rates without systematically increasing N_2O production, even during the transition from oxic to anoxic conditions. Our findings provide new insights into how oxic-anoxic cycling boosts nitrogen metabolism by changing the quantity and quality of organic carbon mobilized from woodchips.

Labile Carbon Release from Oxic-Anoxic Cycling in Woodchip Bioreactors Enhances Nitrate Removal without Increasing Nitrous Oxide Accumulation

Philip M. McGuire[†], Valentina Dai[†], M. Todd Walter[§], and Matthew C. Reid[†*]

[†]School of Civil and Environmental Engineering, Cornell University, Ithaca NY 14853, USA

[§]Department of Biological and Environmental Engineering, Cornell University, Ithaca, NY 14853, USA

*corresponding author: mcr239@cornell.edu

16

17

Abstract

Denitrification in woodchip bioreactors (WBRs) treating agricultural drainage and runoff is frequently carbon-limited due to the recalcitrance of carbon (C) in lignocellulosic woodchip biomass. Recent research has shown that redox fluctuations, achieved through periodic draining and re-flooding of WBRs, can increase nitrate removal rates by enhancing the release of labile C during oxic periods. While dying-rewetting (DRW) cycles appear to hold great promise for improving the performance of denitrifying WBRs, redox fluctuations in nitrogen-rich environments are commonly associated with enhanced emissions of the greenhouse gas nitrous oxide (N_2O) due to inhibition of N_2O reduction in microaerophilic conditions. Here, we evaluate the effects of oxic-anoxic cycling associated with DRW on the quantity and quality of C mobilized from woodchips, nitrate removal rates, and N_2O accumulation in a complementary set of flow-through and batch laboratory bioreactors at 20°C. Redox fluctuations significantly increased nitrate removal rates from 4.8 – 7.2 g N m^{-3} d^{-1} in a continuously saturated (CS) reactor to 9.8-11.2 g N m^{-3} d^{-1} 24 h after a reactor is drained and re-saturated. Results support the theory that DRW conditions lead to faster NO_3^- removal rates by increasing mobilization of labile organic C from woodchips, with lower aromaticity in the dissolved C pool of oxic-anoxic reactors highlighting the importance of lignin breakdown to overall carbon release. There was no evidence for greater N_2O accumulation, measured as N_2O product yields, in the DRW reactors compared to continuously saturated reactors. We propose that greater organic C availability for N_2O reducers following oxic periods outweighs the effect of microaerophilic inhibition of N_2O reduction in controlling N_2O dynamics. Implications of these findings for optimizing DRW cycling to enhance nitrate removal rates in denitrifying WBRs are discussed.

1. Introduction

Woodchip bioreactors (WBRs) are growing in popularity as a sustainable technology for nitrate (NO_3^-) removal from nonpoint sources including agricultural tile drainage[1], stormwater runoff[2], and wastewater effluent[3]. WBRs use lignocellulosic woodchips as a slow-release carbon (C) source and biofilm support structure, and are designed to enhance heterotrophic denitrification at terrestrial-aquatic interfaces and thereby decrease NO_3^- loads to aquatic environments. An estimated 50% of reactive nitrogen (N) derived from anthropogenic land-based activities is transported to coastal waters[4], and there is great interest in the potential of WBRs to control NO_3^- loads to N-limited coastal systems. However, there are concerns regarding the long-term effectiveness of WBRs as the pool of labile woodchip-derived C is depleted[5–8].

Denitrification in NO_3^- rich environments, including WBRs as well as wetlands and riparian zones, is frequently C-limited[5,7,9–12]. In WBRs this is due to the recalcitrance of C in lignin-rich woody biomass[13], particularly in flooded anaerobic conditions where oxidative decomposition processes are inhibited. Readily-hydrolyzed fractions of woodchip C are typically leached from WBRs during the first one to two years of operation, with effluent characterized by dissolved organic carbon (DOC) concentrations of 20 – 80 mg C/L during this period[8,14]. As woodchips age, however, DOC concentrations decrease significantly due to protective lignin sheaths that hinder access to more readily bioavailable cellulosic and hemicellulosic C sources[15]. DOC in a

WBR effluent decreased from 20.7 mg C/L to 3.0 mg C/L over the first 240 days of operation[8] and WBRs older than 2 years are typically characterized by DOC concentrations between 1 - 4 mg C/L[16,17]. This decrease in soluble carbon is observed in conjunction with slower denitrification rates[18]. In addition to diminished NO_3^- removal rates, C-limited conditions in denitrifying environments can also be associated with greater accumulation of nitrous oxide (N_2O)[19,20], an important greenhouse gas and ozone-depleting substance[21]. Efforts to overcome C-limitation in WBRs have included supplemental dosing with exogenous labile C[22–24] but this can be difficult to operationalize in practice in decentralized WBR systems.

Recent research with woodchip media from a 6-year old WBR has demonstrated that periodic redox fluctuations, achieved by drying and rewetting the reactor, increase nitrate removal rates as well as concentrations of total C and DOC concentration in WBR effluent[25,26]. The authors linked the faster NO_3^- removal to greater C bioavailability, presumably driven by enhanced decomposition of woodchip biomass during oxic periods[25,27]. However, other studies did not observe increased NO_3^- removal rates following drying-rewetting of WBRs[28]. While drying-rewetting (DRW) cycles may be beneficial for accelerating denitrification rates in some cases, they are typically associated with enhanced N_2O emissions[29], as the N_2O reductase enzyme, NosZ, is more sensitive to oxygen (O_2) inhibition than upstream N-reducing enzymes that reduce NO_3^- to N_2O[30–33]. This can lead to N_2O accumulation in microaerophilic environments, and

oxic-anoxic cycling in soils often increases N_2O production and emissions[34,35]. A recent study with a WBR experiencing DRW cycles showed an increase in dissolved N_2O concentrations one day after re-saturation[28].

The objective of this study was to clarify the impact of redox fluctuations on coupled N and C metabolisms in WBRs, with a focus on N dynamics in the oxic-anoxic transition following the re-saturation of woodchip media. We originally hypothesized that DRW cycles would increase NO_3^- removal rates by increasing bioavailable C but would simultaneously increase the undesirable production and export of N_2O from WBRs.

2. Materials and Methods

Model Woodchip Bioreactor Flowthrough Experiments. Horizontally oriented laboratory model woodchip bioreactors (1.5 m *length* × 0.1 m *inner diameter*) were constructed in duplicate using PVC pipe with 8 ports for sampling of solutes, including dissolved gases, installed along the length of the reactors (Figures S1-S2). Dissolved oxygen (DO) was measured via needle-type oxygen microsensors (Presens, Germany) inserted through septa at 55 cm ("upstream") and 105 cm ("downstream"). Reactor media consisted of Ash (*Fraxinus* sp.) woodchips collected from a 7-year-old bioreactor treating agricultural tile drainage at the Homer C. Thompson Vegetable Farm in Freeville, New York, USA[36]. The field bioreactor is continuously saturated, with the exception of infrequent, extended dry periods when water levels inside the bioreactor can fall somewhat. Woodchips were rectangular in shape and averaged approximately 4 cm length × 2 cm width × 0.5 cm thickness. Woodchips were packed by hand into the reactors with periodic

shaking to allow woodchips to settle and to facilitate a uniform porosity within and between reactors. Woodchips were maintained in the reactors under fully saturated, continuous flow conditions for 2 months prior to the beginning of the experiments described here. The drainable porosity, equivalent to the effective porosity[37], was determined as the volume of water drained from the woodchip media divided by the woodchip-filled volume of the reactor. The specific retention[17] was determined as the difference in mass between wet and dry woodchips after drying overnight at 105ºC. Both drainable porosity and specific retention were measured from a homogenous mixture from both reactors following the conditioning period but prior to starting the experiment. Total porosity was calculated as the sum of drainable porosity and specific retention. Reactor influent containing 40 mg/L NO_3^- as $NaNO_3$, 2.5 mg/L NH_4^+ as NH_4Cl, and 1.8 mg/L PO_4^{3-} as Na_2HPO_4 at an average pH of 7.7 was fed into the reactors to achieve an approximate hydraulic retention time (HRT) of 12 hours. The influent was not degassed prior to being pumped into the reactor.

5- and 8-week experiments (Experiments 1 and 2, respectively, Table 1) were performed to evaluate the impacts of redox fluctuations on NO_3^- removal rates, N_2O production, and C transformations in each reactor. Experiments were conducted at approximately 20°C, similar to other laboratory bioreactor experiments[16,17] and to temperatures recorded in Central New York bioreactors in late summer ~18°C (data not shown). Each experiment included a continuously saturated (CS) and DRW reactor. Between experiments, woodchips were removed from reactors, homogenized, and redistributed to both reactors to ensure similar starting media. The DRW reactor was subject to weekly drying-rewetting cycles, with 5 days of saturation followed by a 48-h dry period before being reflooded (Figure S3). Reactor drainage took approximately 2

hours. The CS reactor was operated under saturated flow conditions for the duration of the experiments. As woodchips in Experiment 1 and Experiment 2 experienced different antecedent conditions (e.g., approximately half of the woodchips in the continuously-saturated bioreactor in Experiment 2 would have experienced DRW conditions during Experiment 1), these Experiments should not be considered replicates of one another. However, as they are long-term experiments, weekly samplings can be interpreted as replicates of one another.

Bromide (Br^-) tracer tests were used to estimate pore velocity and dispersion via fits to a 1-dimensional advection-dispersion equation:

$$\frac{dc}{dt} = D\frac{d^2c}{dx^2} - v\frac{dc}{dx} \qquad \text{(Eqn. 1)}$$

Where c is the Br^- concentration [M L^{-3}], D is the dispersion coefficient [L^2 T^{-1}], and v is the pore-water velocity [L T^{-1}]. Br^- breakthrough curves were fit using the CXTFIT package of STANMOD[38,39] to estimate v and D. The mean residence time (MRT) associated with each sampling port at a distance L along a reactor was calculated as L/v.

Sample Collection and Analysis. Routine sampling was conducted twice per week, corresponding to 1 day and 4 days after re-flooding of the DRW reactor and collected from ports along the length of the reactor (Figure S1). Water samples were immediately filtered through a 0.22-micron membrane filter prior to analysis via ion chromatography (Thermo Scientific Dionex ICS-2100) and dissolved organic carbon (DOC) using the non-purgeable organic carbon (NPOC) method (Shimadzu TOC-L). Samples were analyzed within one week of collection. Samples for dissolved gas analysis were also collected from reactor ports and were not filtered but preserved in 50 mM sodium azide in 9 mL crimp-sealed vials. A nitrogen (N_2) headspace of

144 approximately 5 mL (actual volume was verified gravimetrically) was introduced, equilibrated
145 with the water by shaking the vial for at least 5 minutes, and analyzed with a gas chromatograph
146 (GC) equipped with an electron capture detector for N_2O and a flame ionization detector for
147 methane (CH_4), with a methanizer for analysis of carbon dioxide (CO_2) (Shimadzu GC-2014).
148 Vials were held at room temperature for no longer than 2 hours prior to N_2 introduction and
149 analyzed within 12 hours of equilibration. In Experiment 2, pH was measured in all samples
150 using a portable pH electrode (Thermo Orion) immediately after samples were collected from the
151 reactor. High frequency sampling, which is characterized by sample collection every few hours
152 immediately following rewetting, was performed during Experiment 2 to examine changes in
153 DO, N species, and carbon during the transition from oxic to anoxic conditions, and the potential
154 for biogeochemical "hot moments" of N_2O production due to microaerophilic conditions[40,41]. In
155 high frequency sampling, only the central four reactor ports (from 36 cm to 125 cm) were
156 sampled for each timepoint.
157
158 NO_3^- removal rates were determined as the slope of a least-squares linear model fit to
159 longitudinal NO_3^- concentration profiles as a function of MRT and then multiplied by the
160 effective porosity of the reactor to report removal rates normalized by total reactor volume. This
161 zero-order modeling of NO_3^- removal rates appropriately describes NO_3^- removal rates under the
162 range of NO_3^- concentrations used here[16,17], though a recent study has questioned the use of zero-
163 order kinetics with influent NO_3^- concentrations < 10 mg NO_3^--N/L[12]. NO_3^- removal efficiency
164 was calculated as:

165 $$NO_3^- \ Removal \ Efficiency = \frac{NO_{3,i}^- - NO_{3,e}^-}{NO_{3,i}^-} \times 100 \quad \text{(Eqn. 2)}$$

166 N_2O production was evaluated as an "effective N_2O yield", with N_2O production along a length
167 of the reactor normalized by the removal of NO_3^- along that length:

168 $$N_2O\ Yield = \frac{N_2O_i - N_2O_0}{-(NO_{3,i}^- - NO_{3,0}^-)} \qquad \text{(Eqn. 3)}$$

169 Where N_2O_i is the N_2O-N concentration at a downstream port *i* [M L^{-3}], N_2O_0 is the N_2O-N
170 concentration in the reactor inlet [M L^{-3}], $NO_{3,i}^-$ is the NO_3^--N concentration at a downstream
171 port *i* [M L^{-3}], and $NO_{3,0}^-$ is the NO_3^--N concentration in the reactor inlet [M L^{-3}]. For high
172 frequency sampling, *i* represents the sampling port at 125 cm, while *o* represents the sampling
173 port at 36 cm.
174
175 Dissolved inorganic carbon (DIC) was determined using headspace GC measurements of CO_2
176 partial pressure in conjunction with pH and carbonate equilibrium models[42]. We assumed that
177 ionic strength effects were negligible.
178 **Woodchip Bioreactor Batch Experiments.** Woodchip batch experiments in 250 mL media
179 bottles were performed with the objective of characterizing effects of antecedent oxic periods on
180 the quantity and quality of organic C mobilized from lignocellulosic woodchips. Media bottles
181 were closed with bromobutyl rubber stoppers to allow liquid to be extracted from anoxic
182 reactors. Ash woodchips, collected from the bioreactor at the Homer C. Thompson Vegetable
183 Farm, were initially incubated in a synthetic media solution of 200 mg/L NO_3^- as $NaNO_3$, 250
184 mg/L KCl, 84 mg/L $NaHCO_3$, 24 mg/L NaH_2PO_4, and a trace element solution (Table S1) for
185 approximately 72 hours in anoxic conditions. 110 g of wet weight woodchips per reactor were
186 then separated into two sets of triplicate batch reactors maintained in the dark. Anoxic reactors
187 were kept permanently anoxic, while oxic-anoxic reactors were aerated for 24 h via air sparging,
188 sealed anoxically for 24 h, aerated for 96 h, sealed anoxically for 48 h, and then aerated for 6

189 days. Following these conditioning steps, both anoxic and oxic-anoxic reactors were decanted,
190 rinsed with the batch reactor synthetic media solution, and then refilled with the batch reactor
191 synthetic media solution. All reactors were sparged with N_2 for 1 hour and then incubated
192 anoxically in the dark with gentle shaking. Samples collected over the next ~120 hours were
193 filtered and analyzed for DOC and for NO_3^- and low molecular weight organic acids via ion
194 chromatography. Samples were collected approximately every 1-2 h for the first 10 h and then
195 sampling was relaxed to 1-2 samples per day for the final ~100 h. Aromaticity of the soluble C
196 pool was assessed via specific ultraviolet absorbance ($SUVA_{254}$)[43]. Absorbance at 254 nm was
197 determined using a UV-Vis spectrophotometer (Shimadzu UV-2600) and was normalized by the
198 DOC concentration.
199
200 **Statistical Methods**. Statistically significant differences among means under different hydraulic
201 regimes were evaluated via one-way ANOVA, Welch one-way ANOVA, or Kruskal-Wallis rank
202 sum tests as appropriate (Table 2). ANOVA assumptions of homogeneity of variance and
203 normality were assessed via Levene's Test and Shapiro-Wilk Test, respectively. Multiple
204 pairwise-comparisons were evaluated using either Tukey's Honest Significant Difference,
205 Games-Howell, or Wilcoxon rank sum post hoc tests. Statistical analyses were implemented in
206 R[44] and evaluated at the 95% confidence level.
207
208 **3. Results**
209 **Bioreactor Hydrodynamics and Redox Cycling.** The effective porosity and specific retention
210 were determined to be 0.58 and 0.31, respectively – similar to previously reported values for
211 woodchip media[45]. Total porosity was 0.89. Mean hydraulic retention times (MRTs) determined

from bromide tracer tests were similar to each other, ranging from 13.4 to 16.0 hours (Table 3, Figures S4-S7). Additional hydraulic parameters are reported in the Electronic Supplementary Information (Table S2). DO concentrations were commonly < 0.1 mg/L in the CS reactor (Figures S8-S11). In the DRW reactor, O_2 levels immediately increased when reactors were drained and the reactor volume filled with atmospheric air. O_2 levels then slowly decreased over the 48-hour dry period before declining quickly (< 2 hrs) to < 0.3 mg/L when reactors were re-saturated and the DO sensors re-submerged (Figures 1 & S12-S14). We acknowledge that the downstream DO sensor in the CS reactor records higher DO concentrations than the upstream sensor, an unexpected result (Figure S9 and S11). This was attributed to a leak in the septum where the "needle-type" microsensor pierces a septum to enter the reactor, so we expect this to be a localized phenomenon that would not impact a large fraction of the reactor.

Nitrogen Transformations. DRW reactors exhibited greater overall mean ± s.d. NO_3^- removal efficiencies, (90.1 ± 11.9 and 94.1 ± 7.8% removal in Experiments 1 and 2, respectively) than CS reactors (46.7 ± 4.2 and 72.9 ± 12.9% removal) (Figures 2A and 2B) and faster NO_3^- removal rates (Figures 2C and 2D). In Experiment 1, mean exported NO_3^- concentrations were 20.20 ± 4.59, 1.09 ± 0.28, and 5.05 ± 3.62 mg/L NO_3^- in CS, DRW 1-day post re-saturation (DRW-1), and DRW 4 days post re-saturation (DRW-4), respectively. Statistically significant differences were observed between CS and DRW-1 ($p = 0.002$) and CS and DRW-4 ($p = 0.002$). Mean exported NO_3^- concentrations between DRW-1 and DRW-4 were not significantly different ($p = 0.151$). In Experiment 2, mean exported NO_3^- concentrations were 12.2 ± 5.70, 0.43 ± 0.40, and 4.79 ± 3.87 mg/L NO_3^- in CS, DRW-1, and DRW-4, respectively. Statistically significant

differences were observed between CS and DRW-1 ($p < 0.001$), CS and DRW-4 ($p = 0.004$), and DRW-1 and DRW-4 ($p = 0.036$).

Mean NO_3^- removal rates are summarized in Table 3. Goodness of fit for linear models of NO_3^- profiles from individual sampling dates was assessed as an adjusted R^2 metric, which ranged between 0.77 – 0.99 and averaged 0.88 across all model fits. In all cases, NO_3^- removal rates were significantly higher in DRW-1 than in CS conditions. In Experiment 1, statistically significant differences were observed between CS and DRW-1 ($p < 0.001$) and CS and DRW-4 ($p < 0.001$), with significantly higher removal rates in the DRW reactors. There was no significant difference in NO_3^- removal rates between DRW-1 and DRW-4 ($p = 0.059$). In Experiment 2, significantly higher removal rates were observed in DRW-1 compared to CS conditions ($p < 0.001$). NO_3^- removal rates between CS and DRW-4 were not significantly different ($p = 0.057$). While NO_3^- removal in DRW reactors were similar in Experiments 1 and 2, NO_3^- removal rates in CS reactors increased from Experiment 1 to 2. This led to smaller differences between DRW and CS reactors in Experiment 2 (Figures 2C and 2D).

N_2O concentration profiles are shown in Figures 3A and 3B, and N_2O yields are summarized in Table 3 and Figures 3C and 3D. The N_2O yield reported in Table 3 is the yield at the reactor port at 135 cm because this represents the dissolved N_2O that would be released in reactor effluent, which is the dominant N_2O release pathway from WBRs[28,46]. N_2O yields were highly variable from week to week, varying by up to 3 orders of magnitude in the same location in the bioreactor in the same experiment. Negative N_2O yields were commonly observed, indicating that at times the reactors served as a net sink of N_2O. This was due to non-zero N_2O in the reactor influent

(Figures 3A and 3B). Analysis of statistically significant differences in N_2O yields was performed by pooling all 5 or 8 weeks of data into "upstream" ports (the first three sampling ports) or "downstream" ports (the final three sampling ports). N_2O yields were generally higher in the upstream sampling ports of the DRW reactor (Figures S15 & S16) than the downstream ports (Figures 3C and 3D), indicating net production of N_2O in upstream portions of the reactor followed by net consumption in downstream portions. In Experiment 1, N_2O yields in downstream ports were significantly higher in the CS reactor than in DRW-1 ($p < 0.001$) and DRW-4 ($p < 0.001$), leading to lower effluent N_2O concentrations in DRW conditions (Figure 3C). There was no significant difference between mean N_2O yields in DRW-1 and DRW-4 ($p = 0.890$). This indicates that, after normalizing N_2O production by the removed concentration of NO_3^--N, there was less production of N_2O in the DRW reactor both 1 and 4 days after re-saturation. In Experiment 2, there was no significant difference in the N_2O yield between the CS and DRW reactors ($p = 0.3$), and similar concentrations of dissolved N_2O were released in reactor effluent (Figure 3B). Similar to the experimental results for nitrate removal rates, there were clearer differences in N_2O production between CS and DRW reactors in Experiment 1 compared to Experiment 2.

Carbon Quantity and Quality. In the CS reactor, DOC concentrations were < 4.0 mg C/L for all sampling ports (Figures 4 and S17). There was little variation in DOC as a function of length within CS reactors, or as a function of time over the five- or eight-week duration of the experiment (Figures S17 and S18). DIC ranged from 9.7-33 mg C/L in CS reactors, and were typically ~15 mg C/L. Dissolved CH_4 concentrations were negligible in the CS reactor throughout the experiment. In the DRW reactor, DOC and DIC exhibited substantial spatial and

280 temporal variability, and in many cases were significantly higher than in the CS reactor (Figures
281 4, S19, and S20). DOC concentrations one day post re-saturation (see example data from Days
282 19 and 40 in Figure 4) in the downstream half of the reactor were usually between 5–7 mg C/L,
283 compared to 2-3 mg C/L in the CS reactor. DOC concentrations were higher in downstream
284 sections of the DRW reactor than upstream portions. By day 4 post re-saturation, DOC
285 concentrations for the most part had decreased to the 2-3 mg C/L range throughout the reactor.
286 DIC concentrations, which reflect the effects of microbial respiration, ranged from 45-65 mg C/L
287 in downstream sections of the DRW reactor on day 1 post re-saturation, decreasing to 20-30 mg
288 C/L on day 4 post re-saturation. Counterintuitively, CH_4 concentrations were higher in the DRW
289 reactor experiencing periodic oxic conditions than the CS reactor. In contrast to DOC and DIC,
290 CH_4 concentrations were similar on days 1 and 4 post re-saturation.
291
292 **Transition from Oxic to Anoxic Conditions.** Results of high-frequency pore water analysis in
293 the 20 h after reactors were re-saturated in Weeks 1, 3, 6, and 8 of Experiment 2 are summarized
294 in Figure 5. In most cases, NO_3^- removal rates across the central 89 cm of the reactor measured
295 during high-frequency analysis were highest immediately following re-saturation and exhibited a
296 declining trend over time. The highest observed NO_3^- removal rate (14.2 g NO_3^--N/m^3-day)
297 occurred during Week 6 and represented an increase of 45% from the mean nitrate removal rate
298 24 h following re-saturation and a 75% increase over the mean 96 h after re-saturation (Table 3).
299 NO_3^- removal rates were elevated immediately after re-saturation despite the presence of
300 elevated DO in upstream portions of the reactor at those times (Figure 5A), and Week 6 was
301 associated with a higher-than-usual DO concentration in the post re-saturation period. NO_3^-
302 removal rates in Week 1 were generally lower than in following weeks and were the only

303 instance in which there was not a clear decline in NO_3^- removal rate as a function of time post re-
304 saturation.
305
306 The effect of the oxic-anoxic transition on effective N_2O yields changed over the course of the
307 experiment. In Weeks 1 and 3, N_2O yields were positive in the period 4 to 10 h after re-flooding
308 and declined as a function of time (Figure 5C). This is consistent with the theory that transient
309 microaerophilic conditions inhibit N_2O reduction and lead to higher N_2O yields. However, in
310 Weeks 6 and 8, N_2O yields exhibited a different pattern, with negative yields in the immediate
311 post re-saturation period increasing over time before converging to yields similar to those
312 observed in Weeks 1 and 3 after 10 h. Notably, Weeks 6 and 8 also had higher DO
313 concentrations in this initial 10 h period than Weeks 1 and 3 (Figure 5A). The change in DIC
314 (ΔDIC) over the central portion of the reactor from 36 to 125 cm was examined to assess
315 whether the negative N_2O yields in Weeks 6 and 8 were associated with signatures of greater C
316 availability than Weeks 1 and 3. Weeks 1, 6, and 8 were all characterized by an increase in
317 ΔDIC over time, indicating an increase in C respiration with time post re-saturation. However,
318 ΔDIC was not consistently greater in Weeks 6 and 8 than Week 1. Week 3 exhibited a different
319 trend, with ΔDIC beginning at a higher level than in the other weeks and decreasing with time.
320 More post re-saturation data up to 80 h for Weeks 3 and 6 as well as additional analysis of
321 correlations among pore water solutes during oxic-anoxic transitions are available in the
322 Electronic Supplementary Information (Figures S21-S28).
323
324 **Batch Reactor Experiments**. A follow-up set of batch reactor experiments was performed to
325 complement flow-through reactor experiments and examine effects of antecedent oxic conditions

on the quality of DOC mobilized from woodchips during subsequent anoxic periods. Woodchip media exposed to oxic-anoxic cycling demonstrated faster overall NO_3^- removal compared to the permanently anoxic reactor (Figure 6A). The oxic-anoxic reactors (OAR) required fewer than 24 hours for complete NO_3^- removal while the anoxic reactors (AR) required at least 76 hours for complete NO_3^- removal.

Carbon release from the OARs greatly exceeded that of the ARs (Figure 6b). After 125 hours, DOC concentrations in the OARs exceeded 100 mg C/L compared to concentrations in the ARs of approximately 30 mg C/L. Quantification of select low molecular weight organic acids (LMWOAs) revealed the dominant LMWOAs to be acetate and propionate. Butyrate was detected but contributed a negligible amount to total DOC. Acetate concentrations began to increase in the OAR after 50 h, while in the AR acetate only began to increase in the final sample, after NO_3^- was fully depleted. Acetate comprised ~35% of the DOC in both the OARs and ARs in later timepoints, while propionate never exceeded 20% of the total DOC. SUVA analysis revealed a significantly lower aromaticity of the DOC pool in the OARs compared to ARs (Figure 6C). In the OARs, SUVA declined by approximately 30% from hour 53 to 126 and was lower than SUVA in the ARs in all the measured samples. In the ARs, SUVA decreased by a factor of nearly 3 in the same timeframe from 2.75 L mg C^{-1} m^{-1} to 0.96 L mg C^{-1} m^{-1}.

4. Discussion

Effects of Drying-Rewetting Cycles on Carbon Release and Nitrate Removal Rates. This study confirms that DRW conditions significantly increase NO_3^- removal rates in WBRs. While this had been shown in some prior work[16,25,26,47], a recent study, using a 54 h dry period in bench

top WBRs, did not observe an increase in NO_3^- removal rates following repeated bioreactor DRW cycles[28]. The lack of a response may have been due to the use of relatively fresh woodchips and correspondingly high DOC levels even in the absence of DRW, or to NO_3^- limitation. Here, we show that NO_3^- removal rates were highest immediately after reactors were re-saturated and decreased from a maximum value of 14.2 g N m^{-3} d^{-1} to 8.1 – 9.6 g N m^{-3} d^{-1} four days after re-saturation. Mean NO_3^- removal rates in CS reactors were 4.8 – 7.2 g N m^{-3} d^{-1}. These rates fall within the range of previously reported values for woodchip bioreactors[16,25]. For example, Maxwell et al. observed mean NO_3^- removal rates of 12.3 and 8.9 g N m^{-3} d^{-1} for DRW and CS reactors, respectively[25]. Maxwell et al. used 8 h dry periods and observed that NO_3^- removal rates in DRW reactors remained higher than rates in CS reactors up to 7 d after reactor re-wetting[25]. Our study produced mixed results on the longevity of enhanced NO_3^- removal rates following a longer 48 h drainage period. In Experiment 1, NO_3^- removal rates 4 d after the dry down were double the rates in the CS reactor, while in Experiment 2 the mean rates in DRW-4 and CS were not significantly different. The lack of a significant difference between CS and DRW-4 in Experiment 2 was largely due to a 50% increase in NO_3^- removal rates in the CS reactor between Experiments 1 and 2. It is possible that the homogenization of woodchips between experiments contributed to this change, since half of the woodchips in the Experiment 2 CS reactor had experienced DRW conditions in Experiment 1, and the effects of antecedent DRW conditions on enhancing woodchip C release may have carried over into the Experiment 2 CS reactor. NO_3^- profiles along the reactor in Experiment 2 exhibited a "kink" at an MRT of approximately 10 hours, which coincided with an increase of DOC and DIC, suggesting a potential role for C release processes in observed increases in NO_3^- removal rates in the latter portion of the column.

There was no evidence for elevated DO concentrations in the oxic-anoxic transition inhibiting NO_3^- reduction. The highest NO_3^- removal rates, usually observed in the first samples collected at roughly 5 h post re-saturation, sometimes had DO levels up to roughly 0.5 mg/L at the upstream DO sensor (Figure 5A). While 0.2 -0.3 mg/L is generally considered to be the O_2 concentration threshold for the onset of denitrification[48], in some aquifer systems this threshold could be as high as 2 mg/L[49,50]. It should be recognized however that the measured O_2 concentrations in this system reflect the DO in the bulk porewater and more anoxic conditions will occur in the denitrifying biofilms. The highest NO_3^- removal rates in the oxic-anoxic transition were observed in Week 6 (Figure 5B), which corresponded to anomalously high DO concentrations at both upstream and downstream DO sensors. This DO anomaly is attributed to the removal of caps on woodchip sampling ports (Fig. S1), for collecting woodchip samples for microbial analyses which will be reported in a forthcoming study.

Our study supports the theory that DRW conditions lead to faster NO_3^- removal rates by increasing soluble C mobilization from woodchips. Total carbon (TC) concentrations in the CS bioreactor of 15 – 30 mg C/L were similar to values reported elsewhere[25], but concentrations in the DRW reactor effluent > 60 mg C/L were greater than those reported before. This may be due to the longer HRTs in our systems (13-16 h) compared to HRTs in the prior study (8 ± 2 h)[23]. Increases in TC along the length of the DRW reactor were primarily driven by changes in DIC, with only small increases in DOC. This suggests that organic C mobilized from woodchips was quickly oxidized to CO_2. The increase in ΔDIC with time after re-saturation observed during most weeks (Figure 5D) suggests that respiration increased as more NO_3^- - rich floodwater

395 flowed through the woodchip media. A notable result in this study was the observation of
396 dissolved CH_4 in the DRW reactors, while concentrations in the CS reactors were negligible.
397 The presence of CH_4 in the bulk fluid one day after re-saturation, and in water samples
398 containing NO_3^- (Figure 2A), points to microbial activity in deeply reducing microenvironments
399 in woodchip-attached biofilms or inside the woodchip[51] in DRW conditions. The lack of DIC
400 and/or CH_4 accumulation in the DRW reactors before the final two water sample points may be
401 due in part to the presence of a headspace in woodchip sampling ports upstream of the final
402 water sample points that could harbor a reservoir of CO_2 or CH_4 (Figures S1 & S2).
403
404 Batch experiments provided further support for links between antecedent oxic conditions, greater
405 organic C mobilization from woodchips, and faster NO_3^- removal rates. Woodchips in the oxic-
406 anoxic reactor released roughly three times as much DOC as the woodchips in the anoxic reactor.
407 There was a notable difference in the aromaticity of the soluble organic carbon pool between the
408 oxic-anoxic and anoxic reactors. Lignin is a phenolic heteropolymer, so the aromatic dissolved
409 C fraction in the bioreactors is most probably derived from lignin. The lower aromaticity in the
410 oxic-anoxic reactor therefore reflects (a) greater oxidative ring-opening of aromatic structures
411 and/or (b) a greater contribution of cellulose- or hemicellulose-derived carbon. Both cases are
412 consistent with the theory that antecedent oxic conditions unlock labile fractions of woodchip
413 carbon.
414
415 **Effects of Drying-Rewetting Cycles on Nitrous Oxide.** We originally hypothesized that
416 drying-rewetting cycles would increase N_2O production in WBRs, particularly in the transition
417 from oxic to anoxic conditions, due to O_2 inhibition of NosZ enzymes. We recently showed that

418 the internal pores of woodchips harbor trapped gas phases after water levels rise in woodchip
419 bioreactors[52], suggesting that O_2 may persist inside woodchips after it is depleted in the bulk
420 fluid and underscoring the potential for drying-rewetting events to lead to microaerophilic
421 conditions inside reactors. Interpretation of differences in N_2O concentrations within WBRs was
422 complicated by non-zero levels of N_2O in the reactor influent (Figure 3A and 3B). This may
423 have resulted from nitrification of NH_4^+ in the reactor influent and was not intentional, but it
424 does represent field conditions, where N_2O produced in soils or in tile drains is introduced to
425 bioreactors[53]. Because of this, we used effective N_2O yields to evaluate the effects of drying-
426 rewetting treatments on N_2O dynamics, since this accounted for the change in N_2O
427 concentrations relative to the influent (Eqn. 3). Results from 1 and 4 days post re-saturation
428 showed that our original hypothesis was not correct. N_2O yields were either lower (Experiment
429 1) or not different (Experiment 2) in DRW reactors compared to CS reactors (Figure 3C and 3D).
430 One explanation for lower N_2O yields is that greater C availability accelerated microbial N_2O
431 reduction along with faster NO_3^- reduction, as has been postulated by Feyereisen et al[23]. While
432 our previous work suggested that water level draw-downs could release N_2O held in trapped gas
433 phases[52], we did not observe this here based on occasional measurements of bioreactor air (data
434 not shown).
435
436 Data from the oxic-anoxic transition showed that in Weeks 1 and 3 there was a transient increase
437 in N_2O yields in the first hours after re-saturation that decreased with time and decreasing DO,
438 consistent with our expectation. However, by Weeks 6 and 8 this pattern reversed, and the
439 immediate post re-saturation period was characterized by low N_2O yields that increased with
440 time and decreasing DO. This difference between early and late phases of the experiment was

not explained by differences in DO, since DO concentrations were higher in Weeks 6 and 8 than 1 and 3 (Figure 5A). One plausible explanation would be that greater C release in the immediate post re-saturation phase of Weeks 6 and 8 accelerated N_2O reduction despite higher DO, perhaps due to a cumulative effect of bioreactor drainage events, but evidence for this is mixed. Weeks 6 and 8 do not exhibit systematically higher ΔDIC than Weeks 1 and 3 in the post re-saturation phase (Figure 5D and S36). However, Week 8 does exhibit significantly higher DOC than all other weeks and Week 6 exhibits significantly higher DOC concentrations than Week 1 (Figure S35). The difference in N_2O yields in the immediate post re-saturation between Weeks 3 and 6 does not persist after 20 h (Figure S23). While figure 5C does reveal that oxic-anoxic transitions may at times lead to transient increases in N_2O yields, a Kruskal-Wallis Rank Sum Test showed that the mean N_2O yields in the period up to 30 h after re-saturation in Weeks 1 and 3 were not significantly greater than the N_2O yields measured in the CS reactor ($p = .092$).

This is among the first studies to evaluate the impact of drying-rewetting conditions on N_2O dynamics in WBRs. Manca et al. recently evaluated N_2O dynamics in WBRs experiencing drying-rewetting cycles and showed that dissolved N_2O concentrations in bench-top WBRs were higher 1 day after re-saturation compared to 3 and 5 days after re-saturation[28]. They did not compare their results in DRW reactors to data in continuously saturated reactors, so the overall effect of DRW cycles on N_2O dynamics was difficult to assess. Our study did not show that DRW cycling increased N_2O yields compared to CS reactors 1 or 4 days post re-saturation, most probably due to greater carbon availability in DRW reactors.

463 The lack of significant enhancement in N_2O accumulation in the transition from oxic to anoxic
464 conditions indicates that greater C availability outweighs inhibitory effects of O_2 and/or that O_2
465 inhibition of N_2O reduction was minor or short-lived. DO concentrations as low as 0.6 mg/L
466 have been shown to significantly inhibit N_2O reduction rates by up to 90% in numerous bacterial
467 strains, with some strains unable to reduce N_2O until DO was completely depleted[54]. DO
468 concentrations at the upstream sensor of the WBRs were in this range up to 10 h after re-
469 saturation in Weeks 6 and 8, and in Week 6 the downstream sensor position was also
470 characterized by DO concentrations in this range (Figure 5A). Notably, Weeks 6 and 8 were also
471 characterized by the lowest N_2O yields, with reactors acting as an N_2O sink (negative N_2O
472 yields) in several cases (Figure 5C). So, there was no clear evidence of a link between
473 microaerophilic O_2 levels and inhibited N_2O reduction in the oxic-anoxic transition even though
474 DO levels observed in the bioreactor have been associated with inhibited N_2O reduction
475 elsewhere. Prior studies have shown that N_2O-reducing microorganisms recover most of their
476 N_2O reducing activity within 1-4 h after O_2 has been depleted[54,55], and this relatively fast
477 recovery may contribute to the lack of N_2O accumulation during the oxic-anoxic transition.
478 While there have been investigations into the microbial community of denitrifying woodchip
479 bioreactors in recent years[20,56–58], there has been little focused study of the N_2O-reducing
480 community, so it is not clear how well the results of pure culture studies translate to the
481 bioreactor community.
482
483 **Implications for Field Operation of Woodchip Bioreactors**. This study suggests that
484 implementation of DRW cycles in woodchip bioreactors has the potential to increase NO_3^-
485 removal rates without increasing N_2O production, and that DRW cycles may, in fact, diminish

N_2O production compared to traditional, continuously saturated conditions. With recent innovations in "smart" water infrastructure[59–61], cost-effective capabilities for automating drying and rewetting of woodchip bioreactors based on sensor feedbacks or precipitation forecasting are in reach. A key need for future research is to determine the optimal duration of dry periods and periodicity of drying-rewetting cycles so as to maximize NO_3^- removal rates while minimizing dry periods when water will be discharged directly to surface waters without treatment. The 8 h dry periods used in Maxwell et al.[25] resulted in comparable increases in NO_3^- removal rate as the 48 h dry periods tested in this study, suggesting that marginal increases in carbon release with time may be small and that shorter dry periods may be optimal[25]. However, in a separate study, Maxwell et al.[16] found that increased durations of 2, 8, and 24-hour drying periods during a weekly cycle produced dramatically higher NO_3^- removal rates with longer unsaturated periods[16]. The effect of the duration of unsaturated periods on C release, and its interaction with variables including woodchip age, temperature[45], and water chemistry, thus remain unclear and merit further attention. Effects of DRW management on N_2O dynamics are also likely to be temperature-dependent, since N_2O reduction rates are thought to be more temperature-sensitive than the reduction rates of upstream nitrogen oxide species[62]. While evaluating effects of HRT variability on N_2O yields was beyond the scope of this study, HRT is a critical determinant on WBR N dynamics[63–65] and other processes[67]. N_2O measurements from Experiment 1 in particular support a conceptual model of net N_2O production followed by net N_2O consumption[66], so it is probable that shorter HRTs could lead to greater N_2O yields if the system effluent is shifted towards the net N_2O production regime.

508 Implementation of DRW management of WBRs will most likely accelerate the depletion of the
509 woodchip media and reduce the effective lifetime of WBRs[13]. Woodchip replacement may
510 significantly contribute to the life cycle cost of WBRs[68], though reports of woodchip replacement
511 costs in the literature are limited. More research is needed to determine the economic trade-offs,
512 from the perspective of life cycle cost per unit NO_3^- removed, incurred by woodchip media
513 replacement. Another concern associated with DRW practices is the direct release of untreated
514 tile drainage during drained periods, but this could be addressed by building parallel bioreactors
515 so that one is always available for treatment.
516
517 Optimizing the benefits of DRW cycling for NO_3^- removal also requires further investigation
518 into the biogeochemical mechanisms driving faster C mobilization from woodchips in DRW
519 conditions. Our study produced novel results that antecedent oxic periods lead to a water-soluble
520 organic C pool with lower aromaticity than a permanently anoxic reactor, highlighting the
521 importance of lignin breakdown and liberation of cellulose and hemicellulose for WBR
522 performance. Fungi are the primary drivers of lignocellulose breakdown in the environment,
523 through oxygen-dependent enzymes or production of reactive oxygen species via Fenton
524 reactions[69]. Both of these pathways would be enhanced by alternating oxic-anoxic conditions in
525 bioreactors. Fungal bioaugmentation could therefore be an important strategy for optimizing
526 WBR performance under DRW cycling. Augmentation with manganese (Mn) may also serve an
527 important role, since Mn has been shown to regulate rates of lignocellulose decay[70,71],
528 presumably due to the role of manganese peroxidase enzymes in lignin breakdown. These
529 processes will require focused study in the context of denitrifying woodchip bioreactors before

530 recommendations on how to optimize reactor biological and chemical properties for enhanced
531 breakdown of lignocellulosic carbon can be made.
532
533 **Author Contributions.** Conceptualization - PMM, MCR, MTW; Data Curation - VD, PMM,
534 MCR; Formal Analysis - PMM, MCR; Funding Acquisition - PMM, MCR, MTW; Investigation
535 - VD, PMM; MCR Methodology - PMM, MCR, MTW; Project Administration - PMM, MCR,
536 MTW; Resources - MCR, MTW; Software - VD, PMM, MCR; Supervision - PMM, MCR,
537 MTW; Validation - VD, PMM, MCR; Visualization - VD, PMM, MCR; Writing - Original Draft
538 - PMM, MCR; Writing - Review & Editing - PMM, MCR, MTW
539
540
541 **Acknowledgements.** This research was funded by NSF award number 1804975. Additional
542 funding was provided by the Cornell Rawlings Presidential Research Scholars Program. The
543 authors thank C. Peterson for assistance with reactor construction, and L. Hurt, V. Starnes, and J.
544 Israel for assistance with bioreactor sampling and maintenance. Data and coding scripts are
545 available online at github.com/ReidLab.
546

Table 1: Experimental Designs and Descriptions

Reactor Design	Replicates and Duration	Experiment Name and Abbreviation	Description
Flowthrough	Two replicates, each with a continuously saturated and a drying-rewetting reactor. The first replicate lasted 5 weeks and the second replicate lasted 8 weeks. There was one drying-rewetting cycle per week in the DRW reactor.	Continuously Saturated (CS)	Reactors were kept under saturated flow conditions for the duration of the experiment.
		Drying-Rewetting (DRW)	Reactors were subjected to weekly draining-reflooding cycles, with 5 days of saturation followed by a 48-hour dry period before being reflooded.
Batch	Triplicate sets of both anoxic and oxic-anoxic reactors operated for 2 weeks	Anoxic Reactor (AR)	Maintained under permanently anoxic conditions.
		Oxic-Anoxic Reactor (OAR)	Aerated for 24 hours via air sparging, sealed anoxically for 24 hours, aerated for 96 hours, sealed anoxically for 48 hours, and then aerated for 6 days

Table 2: Statistical Tool Summary

Examined Metric	Experiment Replicate	ANOVA Assumption Validity		Resulting Statistical Analysis Tool	Post-hoc Test
		Homogeneity of Variance	Normality		
Exported Nitrate	1	X	X	Kruskal-Wallis Rank Sum	Wilcoxon Rank Sum
	2	X	✓	Welch One-Way ANOVA	Games-Howell
Nitrate Removal Rate	1	✓	✓	ANOVA	Tukey
	2	✓	✓	ANOVA	Tukey
N_2O Yield	1	✓	✓	ANOVA	Tukey
	2	X	✓	Welch One-Way ANOVA	N/A: No difference among means

Table 3: Nitrate Removal Rates and N_2O Product Yields

Experiment	Reactor Hydraulic Regime	HRT (h)	Average Temperature (°C)	Average Nitrate Removal Rate (g N/m³-day)	Average Effective N_2O Yield* (mg N_2O-N/ mg NO_3^--N)
Experiment 1	Continuously Saturated (CS)	15.1	19.6	4.8±0.7	$8.1x10^{-3} \pm 2.1x10^{-3}$
	Drying-Rewetting (DRW)	13.4	19.6	1 day post re-saturation (DRW-1): 11.2±0.7	1 day post re-saturation (DRW-1): $1.4x10^{-4} \pm 6.4x10^{-4}$
				4 days post re-saturation (DRW-4): 9.6±1.3	4 days post re-saturation (DRW-4): $-3.6x10^{-4} \pm 5.2x10^{-4}$ †
Experiment 2	Continuously Saturated (CS)	15.2	20.2	7.2±0.9	$-2.7x10^{-4} \pm 2.4x10^{-3}$ †
	Drying-Rewetting (DRW)	16.0	20.2	1 day post re-saturation (DRW-1): 9.8±0.8	1 day post re-saturation (DRW-1): $4.0x10^{-4} \pm 7.1x10^{-4}$
				4 days post re-saturation (DRW-4): 8.1±0.5	4 days post re-saturation (DRW-4): $-7.5x10^{-4} \pm 2.2x10^{-3}$ †

* Calculated using Eqn. 3, where *i* represents the sampling port at 135 cm

† Negative value represents consumption of N_2O between sampling points

References

(1) Christianson, L. E.; Cooke, R. A.; Hay, C. H.; Helmers, M. J.; Feyereisen, G. W.; Ranaivoson, A. Z.; McMaine, J. T.; McDaniel, R.; Rosen, T. R.; Pluer, W. T.; et al. Effectiveness of Denitrifying Bioreactors on Water Pollutant Reduction from Agricultural Areas. *Transactions of the ASABE*. 2021, pp 641–658. https://doi.org/10.13031/TRANS.14011.

(2) Lopez, E. V.; Lynn, T. J.; Peterson, M.; Ergas, S. J.; Trotz, M. A.; Mihelcic, J. R. Enhanced Nutrient Management of Stormwater through a Field Demonstration of Nitrogen Removal in a Modified Bioretention System. In *World Environmental And Water Resources Congress 2016: Environmental, Sustainability, Groundwater, Hydraulic Fracturing, and Water Distribution Systems Analysis - Papers from Sessions of the Proceedings of the 2016 World Environmental and Water Resources* ; 2016. https://doi.org/10.1061/9780784479865.007.

(3) Tanner, C. C.; Sukias, J. P. S.; Headley, T. R.; Yates, C. R.; Stott, R. Constructed Wetlands and Denitrifying Bioreactors for On-Site and Decentralised Wastewater Treatment: Comparison of Five Alternative Configurations. *Ecol. Eng.* **2012**. https://doi.org/10.1016/j.ecoleng.2012.01.022.

(4) Institute for Environment and Sustainability (Joint Research Centre). *Managing Nitrogen and Phosphorus Loads to Water Bodies-Characterisation and Solutions: Towards Macro-Regional Integrated Nutrient Management*; 2014. https://doi.org/10.2788/14322.

(5) Warneke, S.; Schipper, L. A.; Matiasek, M. G.; Scow, K. M.; Cameron, S.; Bruesewitz, D. A.; McDonald, I. R. Nitrate Removal, Communities of Denitrifiers and Adverse Effects in Different Carbon Substrates for Use in Denitrification Beds. *Water Res.* **2011**. https://doi.org/10.1016/j.watres.2011.08.007.

(6) Hu, R.; Zheng, X.; Zheng, T.; Xin, J.; Wang, H.; Sun, Q. Effects of Carbon Availability in a Woody Carbon Source on Its Nitrate Removal Behavior in Solid-Phase Denitrification. *J. Environ. Manage.* **2019**. https://doi.org/10.1016/j.jenvman.2019.06.057.

(7) Roser, M. B.; Feyereisen, G. W.; Spokas, K. A.; Mulla, D. J.; Strock, J. S.; Gutknecht, J. Carbon Dosing Increases Nitrate Removal Rates in Denitrifying Bioreactors at Low-Temperature High-Flow Conditions. *J. Environ. Qual.* **2018**. https://doi.org/10.2134/jeq2018.02.0082.

(8) Abusallout, I.; Hua, G. Characterization of Dissolved Organic Carbon Leached from a Woodchip Bioreactor. *Chemosphere* **2017**, *183*, 36–43. https://doi.org/10.1016/j.chemosphere.2017.05.066.

(9) DeLaune, R. D.; Boar, R. R.; Lindau, C. W.; Kleiss, B. A. Denitrification in Bottomland Hardwood Wetland Soils of the Cache River. *Wetlands* **1996**, *16* (3), 309–320. https://doi.org/10.1007/BF03161322.

(10) Hume, N. P.; Fleming, M. S.; Horne, A. J. Denitrification Potential and Carbon Quality of Four Aquatic Plants in Wetland Microcosms. *Soil Sci. Soc. Am. J.* **2002**, *66* (5), 1706–1712. https://doi.org/10.2136/sssaj2002.1706.

(11) Warneke, S.; Schipper, L. A.; Bruesewitz, D. A.; Baisden, W. T. A Comparison of Different Approaches for Measuring Denitrification Rates in a Nitrate Removing Bioreactor. *Water Res.* **2011**, *45* (14), 4141–4151. https://doi.org/10.1016/j.watres.2011.05.027.

(12) Kouanda, A.; Hua, G. Determination of Nitrate Removal Kinetics Model Parameters in

609 Woodchip Bioreactors. *Water Res.* **2021**, *195*, 116974.
610 https://doi.org/10.1016/j.watres.2021.116974.
611 (13) Moorman, T. B.; Parkin, T. B.; Kaspar, T. C.; Jaynes, D. B. Denitrification Activity,
612 Wood Loss, and N2O Emissions over 9 Years from a Wood Chip Bioreactor. *Ecol. Eng.*
613 **2010**. https://doi.org/10.1016/j.ecoleng.2010.03.012.
614 (14) David, M. B.; Gentry, L. E.; Cooke, R. A.; Herbstritt, S. M. Temperature and Substrate
615 Control Woodchip Bioreactor Performance in Reducing Tile Nitrate Loads in East-Central
616 Illinois. *J. Environ. Qual.* **2016**, *45* (3), 822–829. https://doi.org/10.2134/jeq2015.06.0296.
617 (15) Ghane, E.; Feyereisen, G. W.; Rosen, C. J.; Tschirner, U. W. Carbon Quality of Four-
618 Year-Old Woodchips in a Denitrification Bed Treating Agricultural Drainage Water.
619 *Trans. ASABE* **2018**. https://doi.org/10.13031/trans.12642.
620 (16) Maxwell, B. M.; Birgand, F.; Schipper, L. A.; Christianson, L. E.; Tian, S.; Helmers, M.
621 J.; Williams, D. J.; Chescheir, G. M.; Youssef, M. A. Increased Duration of Drying–
622 Rewetting Cycles Increases Nitrate Removal in Woodchip Bioreactors. *Agric. Environ.*
623 *Lett.* **2019**, *4* (1), 190028. https://doi.org/10.2134/ael2019.07.0028.
624 (17) Halaburka, B. J.; Lefevre, G. H.; Luthy, R. G. Evaluation of Mechanistic Models for
625 Nitrate Removal in Woodchip Bioreactors. *Environ. Sci. Technol.* **2017**, *51* (9), 5156–
626 5164. https://doi.org/10.1021/acs.est.7b01025.
627 (18) Robertson, W. D. Nitrate Removal Rates in Woodchip Media of Varying Age. *Ecol. Eng.*
628 **2010**, *36* (11), 1581–1587. https://doi.org/10.1016/j.ecoleng.2010.01.008.
629 (19) Pan, Y.; Ni, B. J.; Bond, P. L.; Ye, L.; Yuan, Z. Electron Competition among Nitrogen
630 Oxides Reduction during Methanol-Utilizing Denitrification in Wastewater Treatment.
631 *Water Res.* **2013**, *47* (10), 3273–3281. https://doi.org/10.1016/j.watres.2013.02.054.
632 (20) Aalto, S. L.; Suurnäkki, S.; von Ahnen, M.; Siljanen, H. M. P.; Pedersen, P. B.; Tiirola,
633 M. Nitrate Removal Microbiology in Woodchip Bioreactors: A Case-Study with Full-
634 Scale Bioreactors Treating Aquaculture Effluents. *Sci. Total Environ.* **2020**, *723*, 138093.
635 https://doi.org/10.1016/j.scitotenv.2020.138093.
636 (21) Ravishankara, A. R.; Daniel, J. S.; Portmann, R. W. Nitrous Oxide (N2O): The Dominant
637 Ozone-Depleting Substance Emitted in the 21st Century. *Science (80-.).* **2009**.
638 https://doi.org/10.1126/science.1176985.
639 (22) Roser, M. B.; Feyereisen, G. W.; Spokas, K. A.; Mulla, D. J.; Strock, J. S.; Gutknecht, J.
640 Carbon Dosing Increases Nitrate Removal Rates in Denitrifying Bioreactors at Low-
641 Temperature High-Flow Conditions. *J. Environ. Qual.* **2018**, *47* (4), 856–864.
642 https://doi.org/10.2134/jeq2018.02.0082.
643 (23) Feyereisen, G. W.; Spokas, K. A.; Strock, J. S.; Mulla, D. J.; Ranaivoson, A. Z.; Coulter,
644 J. A. Nitrate Removal and Nitrous Oxide Production from Upflow and Downflow Column
645 Woodchip Bioreactors. *Agric. Environ. Lett.* **2020**, *5* (1), e20024.
646 https://doi.org/10.1002/ael2.20024.
647 (24) Jansen, S.; Stuurman, R.; Chardon, W.; Ball, S.; Rozemeijer, J.; Gerritse, J. Passive
648 Dosing of Organic Substrates for Nitrate-Removing Bioreactors Applied in Field Margins.
649 *J. Environ. Qual.* **2019**, *48* (2), 394–402. https://doi.org/10.2134/jeq2018.04.0165.
650 (25) Maxwell, B. M.; Birgand, F.; Schipper, L. A.; Christianson, L. E.; Tian, S.; Helmers, M.
651 J.; Williams, D. J.; Chescheir, G. M.; Youssef, M. A. Drying-Rewetting Cycles Affect
652 Nitrate Removal Rates in Woodchip Bioreactors. *J. Environ. Qual.* **2019**, *48* (1), 93–101.
653 https://doi.org/10.2134/jeq2018.05.0199.
654 (26) Maxwell, B. M.; Diáz-Garciá, C.; Martínez-Sánchez, J. J.; Birgand, F.; Álvarez-Rogel, J.

Temperature Sensitivity of Nitrate Removal in Woodchip Bioreactors Increases with Woodchip Age and Following Drying-Rewetting Cycles. *Environ. Sci. Water Res. Technol.* **2020**, *6* (10), 2752–2765. https://doi.org/10.1039/d0ew00507j.

(27) Christianson, L. E.; Lepine, C.; Sibrell, P. L.; Penn, C.; Summerfelt, S. T. Denitrifying Woodchip Bioreactor and Phosphorus Filter Pairing to Minimize Pollution Swapping. *Water Res.* **2017**. https://doi.org/10.1016/j.watres.2017.05.026.

(28) Manca, F.; De Rosa, D.; Reading, L. P.; Rowlings, D. W.; Scheer, C.; Schipper, L. A.; Grace, P. R. Effect of Soil Cap and Nitrate Inflow on Nitrous Oxide Emissions from Woodchip Bioreactors. *Ecol. Eng.* **2021**, *166*, 106235. https://doi.org/10.1016/j.ecoleng.2021.106235.

(29) Guo, X.; Drury, C. F.; Yang, X.; Reynolds, W. D.; Fan, R. The Extent of Soil Drying and Rewetting Affects Nitrous Oxide Emissions, Denitrification, and Nitrogen Mineralization. *Soil Sci. Soc. Am. J.* **2014**, *78* (1), 194–204. https://doi.org/10.2136/SSSAJ2013.06.0219.

(30) Arai, H.; Mizutani, M.; Igarashi, Y. Transcriptional Regulation of the Nos Genes for Nitrous Oxide Reductase in Pseudomonas Aeruginosa. *Microbiology* **2003**, *149* (1), 29–36. https://doi.org/10.1099/mic.0.25936-0.

(31) Korner, H.; Zumft, W. G. Expression of Denitrification Enzymes in Response to the Dissolved Oxygen Levels and Respiratory Substrate in Continuous Culture of Pseudomonas Stutzeri. *Appl. Environ. Microbiol.* **1989**.

(32) Zumft, W. G. Cell Biology and Molecular Basis of Denitrification. *Microbiol. Mol. Biol. Rev.* **1997**, *61* (4), 533–616.

(33) Ni, B. J.; Ruscalleda, M.; Pellicer-Nàcher, C.; Smets, B. F. Modeling Nitrous Oxide Production during Biological Nitrogen Removal via Nitrification and Denitrification: Extensions to the General ASM Models. *Environ. Sci. Technol.* **2011**. https://doi.org/10.1021/es201489n.

(34) Pandey, A.; Mai, V. T.; Vu, D. Q.; Bui, T. P. L.; Mai, T. L. A.; Jensen, L. S.; de Neergaard, A. Organic Matter and Water Management Strategies to Reduce Methane and Nitrous Oxide Emissions from Rice Paddies in Vietnam. *Agric. Ecosyst. Environ.* **2014**. https://doi.org/10.1016/j.agee.2014.06.010.

(35) Linquist, B. A.; Anders, M. M.; Adviento-Borbe, M. A. A.; Chaney, R. L.; Nalley, L. L.; da Rosa, E. F. F.; van Kessel, C. Reducing Greenhouse Gas Emissions, Water Use, and Grain Arsenic Levels in Rice Systems. *Glob. Chang. Biol.* **2015**. https://doi.org/10.1111/gcb.12701.

(36) Hassanpour, B.; Giri, S.; Pluer, W. T.; Steenhuis, T. S.; Geohring, L. D. Seasonal Performance of Denitrifying Bioreactors in the Northeastern United States: Field Trials. *J. Environ. Manage.* **2017**, *202* (1), 242–253. https://doi.org/10.1016/j.jenvman.2017.06.054.

(37) Ghane, E.; Feyereisen, G. W.; Rosen, C. J. Efficacy of Bromide Tracers for Evaluating the Hydraulics of Denitrification Beds Treating Agricultural Drainage Water. *J. Hydrol.* **2019**. https://doi.org/10.1016/j.jhydrol.2019.02.031.

(38) Simunek, J.; van Genuchten, M. T.; Sejna, M.; Toride, N.; Leij, F. J. The STANMOD Computer Software for Evaluating Solute Transport in Porous Media Using Analytical Solutions of Convection-Dispersion Equation. *Agriculture* **1999**.

(39) Van Genuchten, M. T.; Šimůnek, J.; Leij, F. J.; Toride, N.; Šejna, M. STANMOD: Model Use, Calibration, and Validation. *Trans. ASABE* **2012**, *55* (4), 1353–1366.

(40) McClain, M. E.; Boyer, E. W.; Dent, C. L.; Gergel, S. E.; Grimm, N. B.; Groffman, P. M.; Hart, S. C.; Harvey, J. W.; Johnston, C. A.; Mayorga, E.; et al. Biogeochemical Hot Spots

and Hot Moments at the Interface of Terrestrial and Aquatic Ecosystems. *Ecosystems* **2003**, *6* (4), 301–312. https://doi.org/10.1007/s10021-003-0161-9.

(41) Groffman, P. M.; Butterbach-Bahl, K.; Fulweiler, R. W.; Gold, A. J.; Morse, J. L.; Stander, E. K.; Tague, C.; Tonitto, C.; Vidon, P. Challenges to Incorporating Spatially and Temporally Explicit Phenomena (Hotspots and Hot Moments) in Denitrification Models. *Biogeochemistry* **2009**. https://doi.org/10.1007/s10533-008-9277-5.

(42) Morel, Francois, M. M.; Hering, J. G. *Principles and Applications of Aquatic Chemistry*; John Wiley & Sons, 1993.

(43) Weishaar, J. L.; Aiken, G. R.; Bergamaschi, B. A.; Fram, M. S.; Fujii, R.; Mopper, K. Evaluation of Specific Ultraviolet Absorbance as an Indicator of the Chemical Composition and Reactivity of Dissolved Organic Carbon. *Environ. Sci. Technol.* **2003**, *37* (20), 4702–4708. https://doi.org/10.1021/es030360x.

(44) R Core Team. *R: A Language and Environment for Statistical Computing*; 2021. https://doi.org/10.1007/978-3-540-74686-7.

(45) Halaburka, B. J.; Lefevre, G. H.; Luthy, R. G. Quantifying the Temperature Dependence of Nitrate Reduction in Woodchip Bioreactors: Experimental and Modeled Results with Applied Case-Study. *Environ. Sci. Water Res. Technol.* **2019**, *5* (4), 782–797. https://doi.org/10.1039/c8ew00848e.

(46) Warneke, S.; Schipper, L. A.; Bruesewitz, D. A.; McDonald, I.; Cameron, S. Rates, Controls and Potential Adverse Effects of Nitrate Removal in a Denitrification Bed. *Ecol. Eng.* **2011**. https://doi.org/10.1016/j.ecoleng.2010.12.006.

(47) Hua, G.; Salo, M. W.; Schmit, C. G.; Hay, C. H. Nitrate and Phosphate Removal from Agricultural Subsurface Drainage Using Laboratory Woodchip Bioreactors and Recycled Steel Byproduct Filters. *Water Res.* **2016**. https://doi.org/10.1016/j.watres.2016.06.022.

(48) Seitzinger, S.; Harrison, J. A.; Böhlke, J. K.; Bouwman, A. F.; Lowrance, R.; Peterson, B.; Tobias, C.; Van Drecht, G. Denitrification across Landscapes and Waterscapes: A Synthesis. *Ecological Applications*. 2006, pp 2064–2090. https://doi.org/10.1890/1051-0761(2006)016[2064:DALAWA]2.0.CO;2.

(49) McMahon, P. B.; Böhlke, J. K.; Christenson, S. C. Geochemistry, Radiocarbon Ages, and Paleorecharge Conditions along a Transect in the Central High Plains Aquifer, Southwestern Kansas, USA. *Appl. Geochemistry* **2004**, *19* (11), 1655–1686. https://doi.org/10.1016/J.APGEOCHEM.2004.05.003.

(50) Böhlke, J. K.; Wanty, R.; Tuttle, M.; Delin, G.; Landon, M. Denitrification in the Recharge Area and Discharge Area of a Transient Agricultural Nitrate Plume in a Glacial Outwash Sand Aquifer, Minnesota. *Water Resour. Res.* **2002**, *38* (7), 10–11. https://doi.org/10.1029/2001WR000663.

(51) Lopez-Ponnada, E. V; Lynn, T. J.; Peterson, M.; Ergas, S. J.; Mihelcic, J. R. Application of Denitrifying Wood Chip Bioreactors for Management of Residential Non-Point Sources of Nitrogen. *J. Biol. Eng.* **2017**, *11* (1). https://doi.org/10.1186/s13036-017-0057-4.

(52) McGuire, P. M.; Reid, M. C. Nitrous Oxide and Methane Dynamics in Woodchip Bioreactors: Effects of Water Level Fluctuations on Partitioning into Trapped Gas Phases. *Environ. Sci. Technol.* **2019**, *53* (24), 14348–14356. https://doi.org/10.1021/acs.est.9b04829.

(53) Davis, M. P.; Martin, E. A.; Moorman, T. B.; Isenhart, T. M.; Soupir, M. L. Nitrous Oxide and Methane Production from Denitrifying Woodchip Bioreactors at Three Hydraulic Residence Times. *J. Environ. Manage.* **2019**, *242*, 290–297.

https://doi.org/10.1016/j.jenvman.2019.04.055.
(54) Suenaga, T.; Riya, S.; Hosomi, M.; Terada, A. Biokinetic Characterization and Activities of N2O-Reducing Bacteria in Response to Various Oxygen Levels. *Front. Microbiol.* **2018**, *9*, 697. https://doi.org/10.3389/fmicb.2018.00697.
(55) Zhou, Y.; Suenaga, T.; Qi, C.; Riya, S.; Hosomi, M.; Terada, A. Temperature and Oxygen Level Determine N2O Respiration Activities of Heterotrophic N2O-Reducing Bacteria: Biokinetic Study. *Biotechnol. Bioeng.* **2021**, *118* (3), 1330–1341. https://doi.org/10.1002/bit.27654.
(56) Jang, J.; Anderson, E. L.; Venterea, R. T.; Sadowsky, M. J.; Rosen, C. J.; Feyereisen, G. W.; Ishii, S. Denitrifying Bacteria Active in Woodchip Bioreactors at Low-Temperature Conditions. *Front. Microbiol.* **2019**. https://doi.org/10.3389/fmicb.2019.00635.
(57) van der Lelie, D.; Taghavi, S.; McCorkle, S. M.; Li, L. L.; Malfatti, S. A.; Monteleone, D.; Donohoe, B. S.; Ding, S. Y.; Adney, W. S.; Himmel, M. E.; et al. The Metagenome of an Anaerobic Microbial Community Decomposing Poplar Wood Chips. *PLoS One* **2012**, *7* (5), e36740. https://doi.org/10.1371/journal.pone.0036740.
(58) Hellman, M.; Hubalek, V.; Juhanson, J.; Almstrand, R.; Peura, S.; Hallin, S. Substrate Type Determines Microbial Activity and Community Composition in Bioreactors for Nitrate Removal by Denitrification at Low Temperature. *Sci. Total Environ.* **2021**, *755*, 143023. https://doi.org/10.1016/j.scitotenv.2020.143023.
(59) Troutman, S. C.; Love, N. G.; Kerkez, B. Balancing Water Quality and Flows in Combined Sewer Systems Using Real-Time Control. *Environ. Sci. Water Res. Technol.* **2020**, *6* (5), 1357–1369. https://doi.org/10.1039/c9ew00882a.
(60) Kerkez, B.; Gruden, C.; Lewis, M.; Montestruque, L.; Quigley, M.; Wong, B.; Bedig, A.; Kertesz, R.; Braun, T.; Cadwalader, O.; et al. Smarter Stormwater Systems. *Environ. Sci. Technol.* **2016**. https://doi.org/10.1021/acs.est.5b05870.
(61) Bartos, M.; Wong, B.; Kerkez, B. Open Storm: A Complete Framework for Sensing and Control of Urban Watersheds. *Environ. Sci. Water Res. Technol.* **2018**, *4* (3), 346–358. https://doi.org/10.1039/c7ew00374a.
(62) Holtan-Hartwig, L.; Dörsch, P.; Bakken, L. R. Low Temperature Control of Soil Denitrifying Communities: Kinetics of N2O Production and Reduction. *Soil Biol. Biochem.* **2002**, *34* (11), 1797–1806. https://doi.org/10.1016/S0038-0717(02)00169-4.
(63) Greenan, C. M.; Moorman, T. B.; Parkin, T. B.; Kaspar, T. C.; Jaynes, D. B. Denitrification in Wood Chip Bioreactors at Different Water Flows. *J. Environ. Qual.* **2009**, *38* (4), 1664–1671. https://doi.org/10.2134/jeq2008.0413.
(64) Hoover, N. L.; Bhandari, A.; Soupir, M. L.; Moorman, T. B. Woodchip Denitrification Bioreactors: Impact of Temperature and Hydraulic Retention Time on Nitrate Removal. *This Artic. is from J. Enivronmental Qual.* **2016**, *45*, 803–812. https://doi.org/10.2134/jeq2015.03.0161.
(65) Pluer, W. T.; Morris, C. K.; Walter, M. T.; Geohring, L. D. Denitrifying Bioreactor Response during Storm Events. *Agric. Water Manag.* **2019**, *213*, 1109–1115. https://doi.org/10.1016/J.AGWAT.2018.12.004.
(66) Quick, A. M.; Reeder, W. J.; Farrell, T. B.; Tonina, D.; Feris, K. P.; Benner, S. G. Controls on Nitrous Oxide Emissions from the Hyporheic Zones of Streams. *Environ. Sci. Technol.* **2016**. https://doi.org/10.1021/acs.est.6b02680.
(67) Rivas, A.; Barkle, G.; Stenger, R.; Moorhead, B.; Clague, J. Nitrate Removal and Secondary Effects of a Woodchip Bioreactor for the Treatment of Subsurface Drainage

with Dynamic Flows under Pastoral Agriculture. *Ecol. Eng.* **2020**, *148*, 105786. https://doi.org/10.1016/j.ecoleng.2020.105786.
(68) Lepine, C.; Christianson, L.; Davidson, J.; Summerfelt, S. Woodchip Bioreactors as Treatment for Recirculating Aquaculture Systems' Wastewater: A Cost Assessment of Nitrogen Removal. *Aquac. Eng.* **2018**. https://doi.org/10.1016/j.aquaeng.2018.09.001.
(69) Cragg, S. M.; Beckham, G. T.; Bruce, N. C.; Bugg, T. D. H.; Distel, D. L.; Dupree, P.; Etxabe, A. G.; Goodell, B. S.; Jellison, J.; McGeehan, J. E.; et al. Lignocellulose Degradation Mechanisms across the Tree of Life. *Curr. Opin. Chem. Biol.* **2015**, *29*, 108–119. https://doi.org/10.1016/j.cbpa.2015.10.018.
(70) Keiluweit, M.; Nico, P.; Harmon, M. E.; Mao, J.; Pett-Ridge, J.; Kleber, M. Long-Term Litter Decomposition Controlled by Manganese Redox Cycling. *Proc. Natl. Acad. Sci. U. S. A.* **2015**, *112* (38), E5253–E5260. https://doi.org/10.1073/pnas.1508945112.
(71) Jones, M. E.; Nico, P. S.; Ying, S.; Regier, T.; Thieme, J.; Keiluweit, M. Manganese-Driven Carbon Oxidation at Oxic-Anoxic Interfaces. *Environ. Sci. Technol.* **2018**, *52* (21), 12349–12357. https://doi.org/10.1021/acs.est.8b03791.

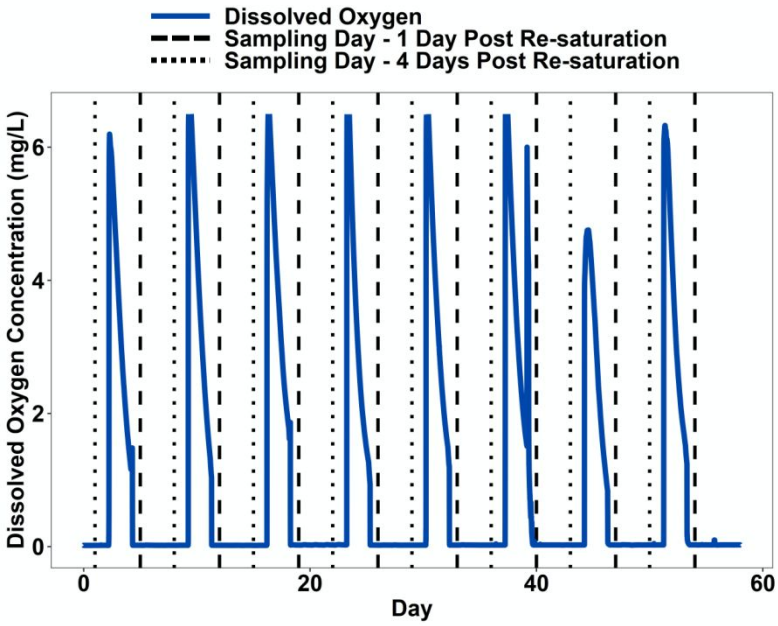

Figure 1: Dissolved oxygen (DO) concentrations at the downstream DO sensor in the drying-rewetting bioreactor of Experiment 2. The dashed and dotted lines indicate the timing of pore water sampling 1 (DRW-1) and 4 (DRW-4) days after reactor re-saturation.

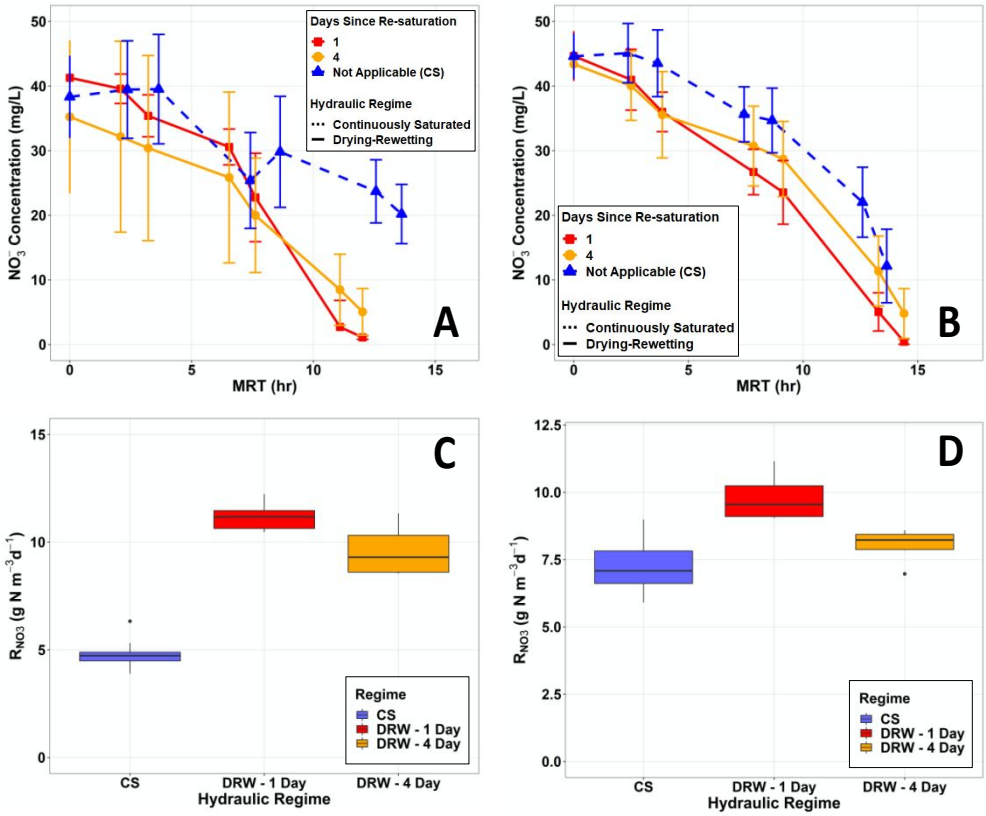

Figure 2: (A, B) Nitrate profiles along the length of reactors. The x-axis represents distinct sampling ports, with mean residence time (MRT) determined as length along the reactor/porewater velocity. The differences in sample MRTs between CS and DRW reactors occurs because of slightly different porewater velocities. Symbols show mean values and error bars show standard deviation. (C, D) Nitrate removal rates under varying hydraulic conditions. Panels (A) and (C) are from Experiment 1. Panels (B) and (D) are from Experiment 2.

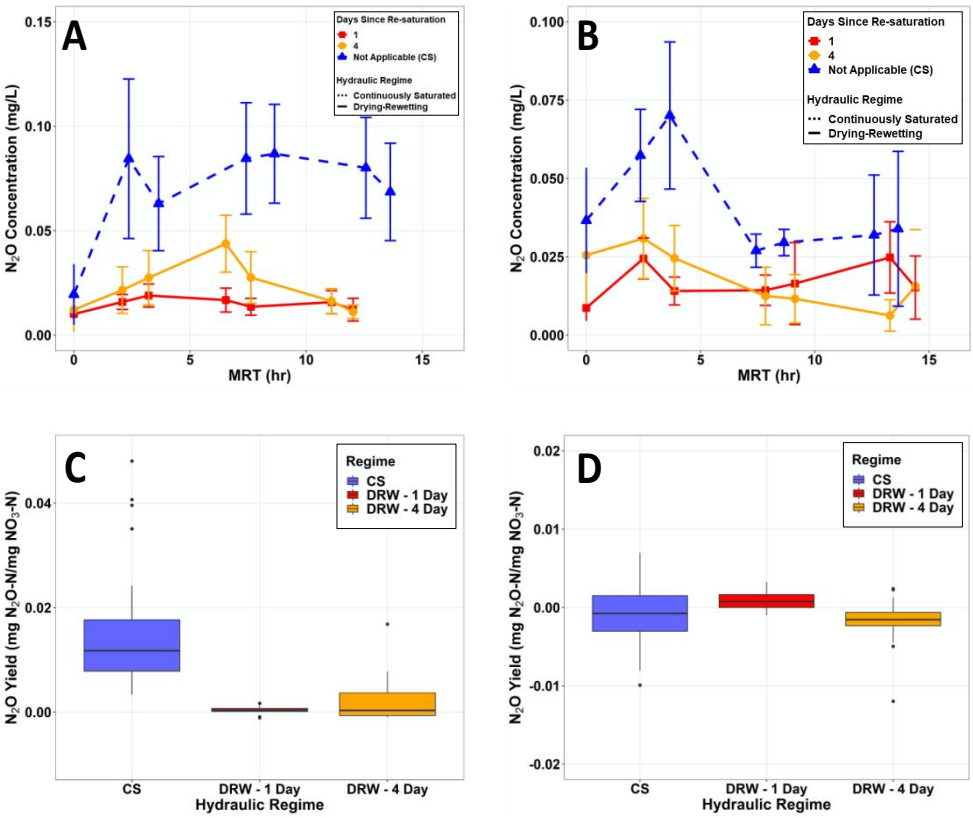

Figure 3: (A, B) Dissolved nitrous oxide (N_2O) profiles in different hydraulic regimes. The x-axis represents distinct sampling ports, with mean residence time (MRT) determined as length along the reactor/porewater velocity. The differences in sample MRTs between CS and DRW reactors occurs because of slightly different hydraulic retention times in the two reactors. Symbols show mean values and error bars show standard deviation. (C, D) Effective N_2O yields in downstream sampling ports (ports located at 0.86, 1.25, and 1.35 m), as defined in Eq. 3. Panels (A) and (C) are from Experiment 1. Panels (B) and (D) are from Experiment 2.

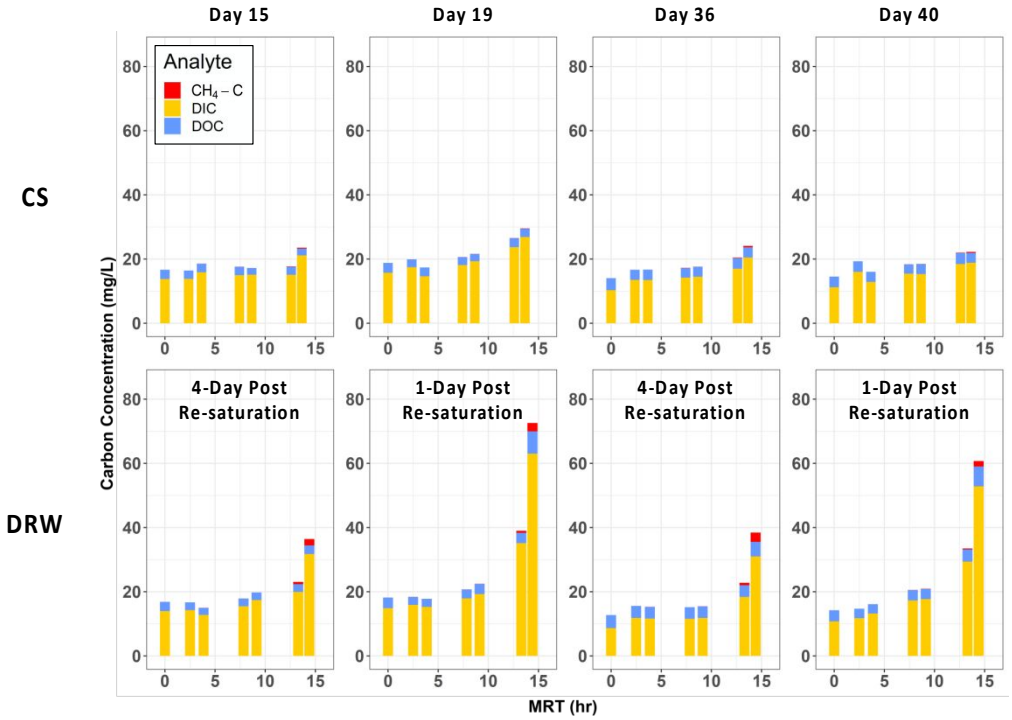

838

839 **Figure 4**: Profiles of dissolved inorganic carbon (DIC), dissolved organic carbon (DOC), and methane
840 (CH_4-C) from select sampling days in continuously saturated (CS) and drying-rewetting (DRW) reactors.
841 Each bar represents a discrete water sampling port, with mean residence time (MRT) determined as length
842 along the reactor/porewater velocity.

843

844

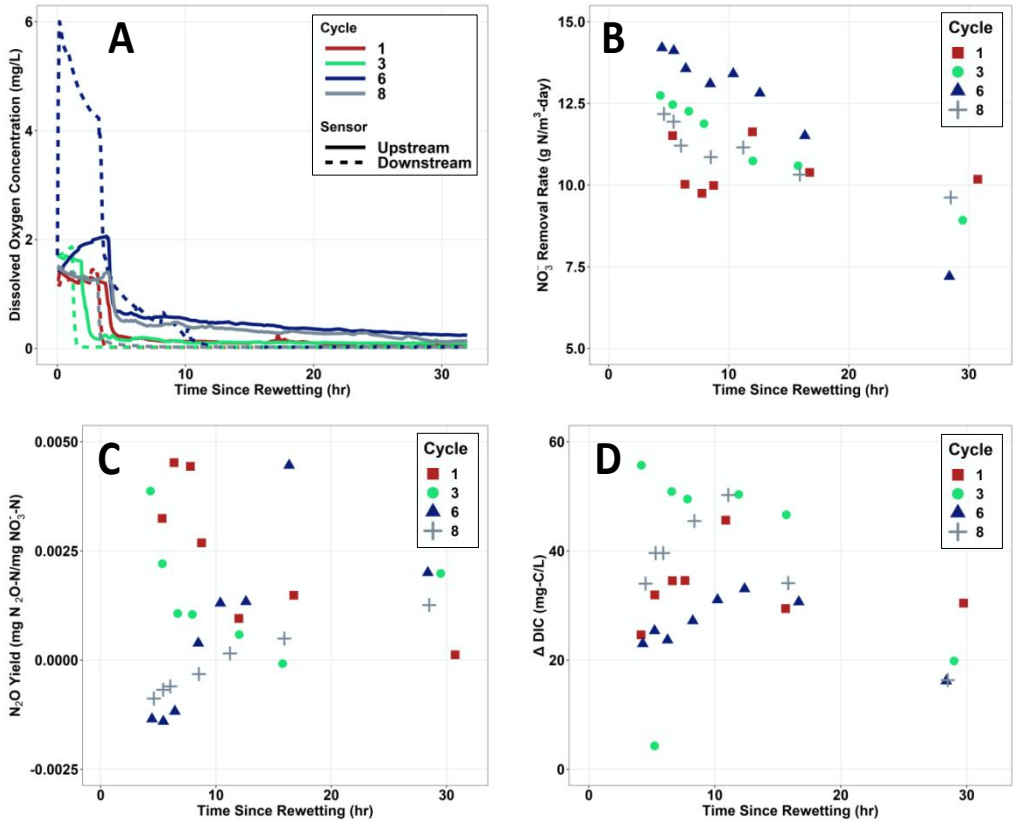

Figure 5: Porewater chemistry immediately following reactor rewetting during drying-rewetting (DRW) cycles 1, 3, 6, and 8. The x-axis represents the time of sampling relative to the re-flooding of the DRW reactor. The first samples were collected at roughly 5 h post re-saturation because it took 5 h for the water level to reach the sampling ports. Time 0 represents the start of rewetting. (A) Dissolved oxygen concentrations at upstream and downstream sensors; (B) Nitrate removal rates; (C) Effective nitrous oxide yields; (D) Change in dissolved inorganic carbon (ΔDIC) from sampling location at 36 to 125 cm at each time point.

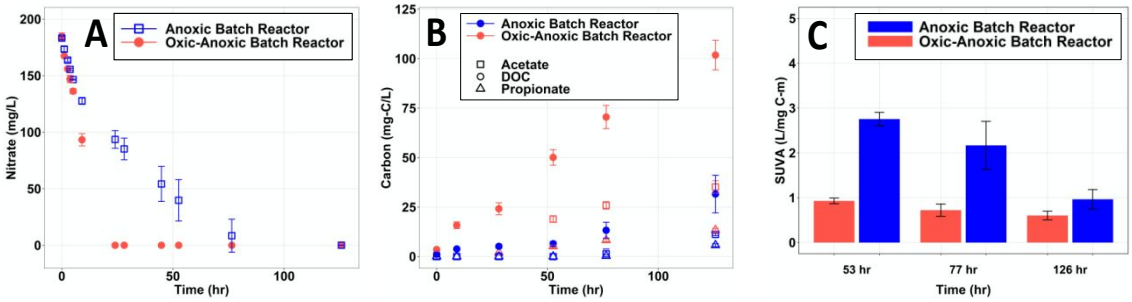

861

862 **Figure 6**: Aqueous nitrate removal and carbon quantity and quality in woodchip batch reactors
863 conditioned under anoxic or oxic-anoxic conditions. At time 0, batch reactors were supplied with a fresh
864 nutrient solution and all reactors were incubated anoxically. Symbols or bars show mean values and error
865 bars show the standard deviation of n=3 reactors (A) Nitrate removal; (B) Mobilization of dissolved
866 organic carbon and low molecular weight organic acids into solution; (C) Specific ultraviolet absorbance
867 (SUVA) at three different time points.

868